

## Supplementary Information Available

### Graphene Oxide Nanosheets Augment Silk Fibroin Aerogels for Enhanced Water Stability and Oil Adsorption

Catherine E. Machnicki, Eric M. DuBois, Meg Fay, Snehi Shrestha, Zachary S. S. L. Saleeba, Alex M. Hruska, Zahra Ahmed, Vikas Srivastava, Po-Yen Chen, and Ian Y. Wong

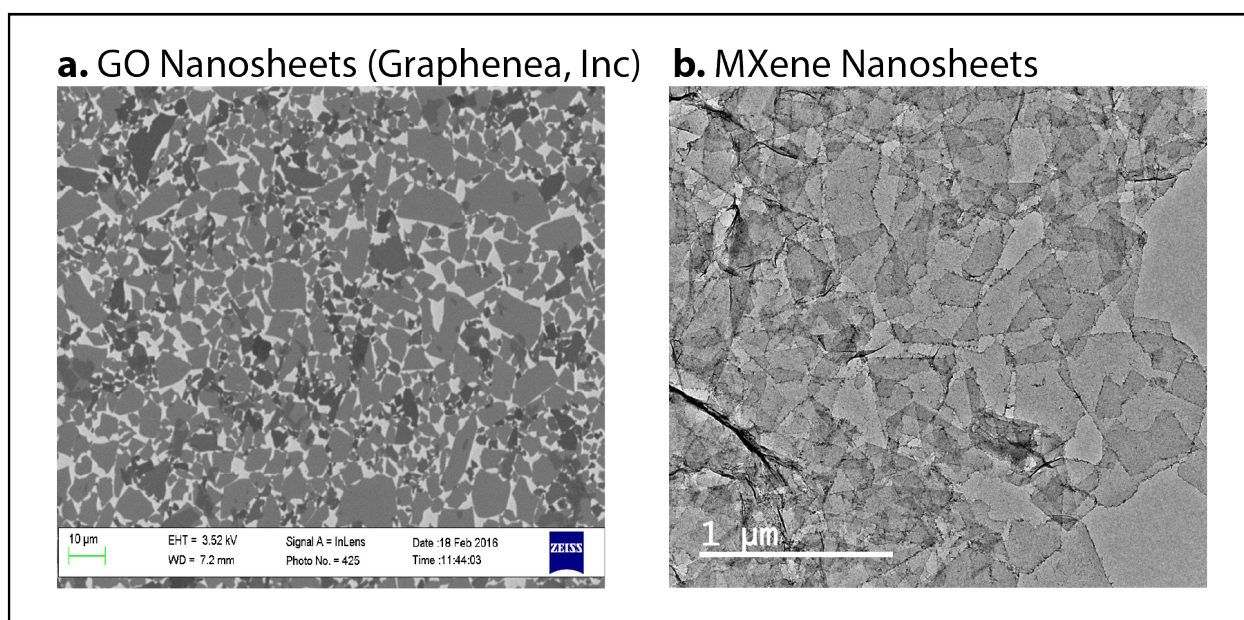


Figure S1: a) Representative SEM image of GO nanosheets (provided by Graphenea, Inc. <https://www.graphenea.com/collections/graphene-oxide/products/graphene-oxide-4-mg-ml-water-dispersion-1000-ml>). b) Representative TEM of MXene nanosheets.

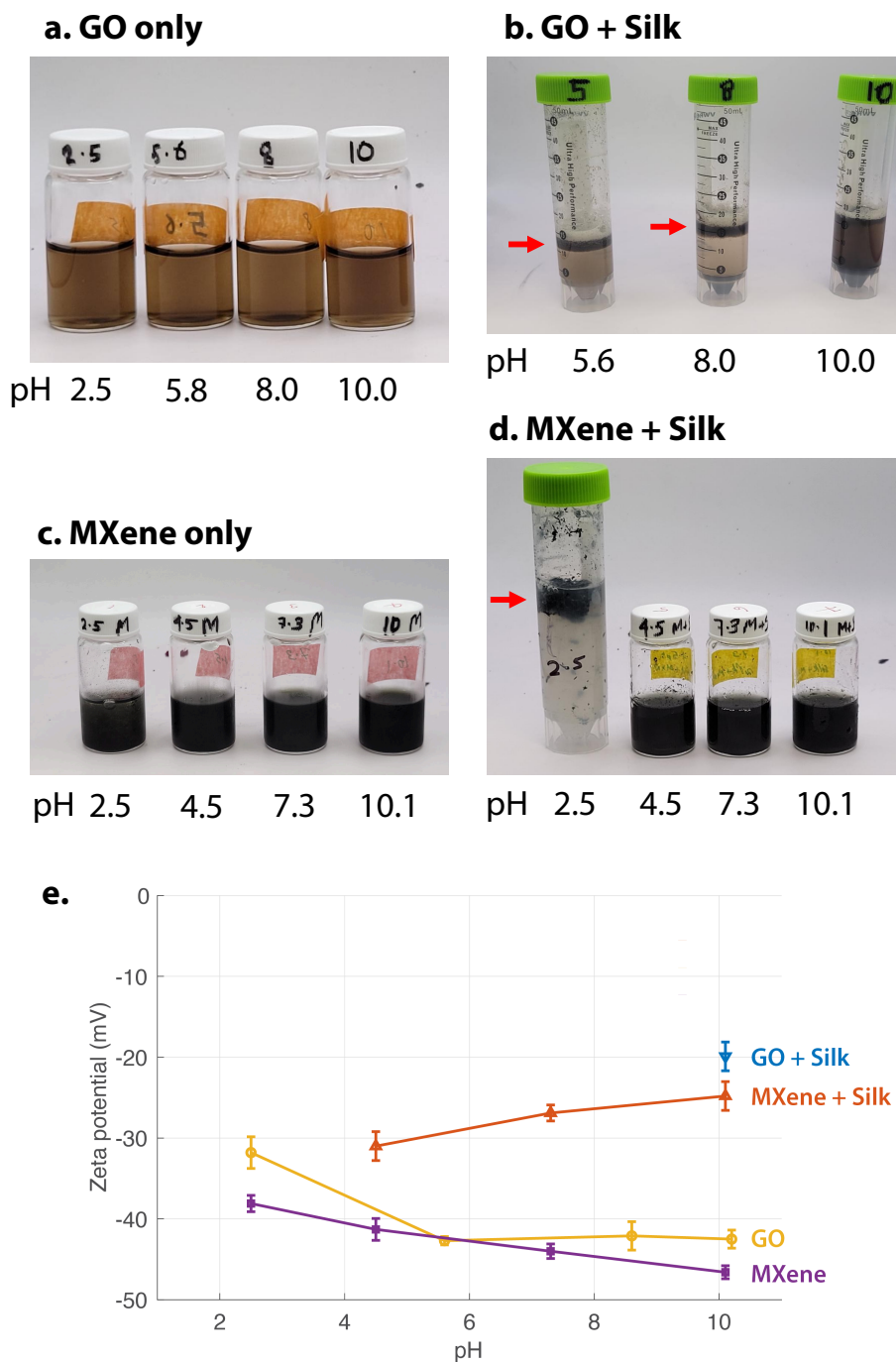


Figure S2: Dispersion of silk fibroin and 2D material nanosheets in water at varying pH, showing greater stability at pH 10. (a) 2 mg/mL graphene oxide, (b) 2 mg/mL graphene oxide with 20 mg/mL silk fibroin, (c) 2 mg/mL MXene, (d) 2 mg/mL MXene with 20 mg/mL silk fibroin. Red arrows denote aggregated conditions. (e) Zeta potential of various silk fibroin and 2D material mixtures, with  $N = 3$  experimental replicates. Markers denote mean and error bars indicate standard deviation. Aggregated solutions at low pH were not characterized.

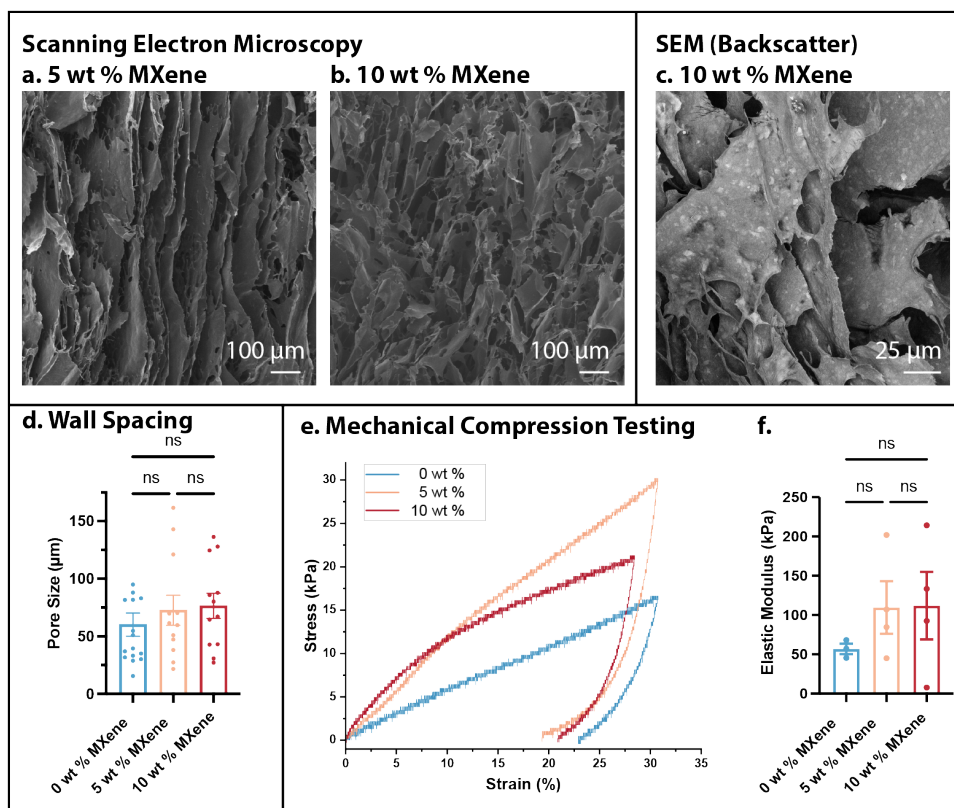


Figure S3: Microstructure and mechanical characterization of Silk-MXene aerogels. (a,b) Representative cross-sectional SEM images at 5 wt % MXene and 10 wt % MXene. (c) Electrical conductivity of 10 wt % MXene aerogels imaged through directional backscatter mode in SEM. (d) Comparison of lateral wall separation as a readout of pore size. (e) Representative stress-strain curve of silk-MXene aerogels. (f) Elastic modulus and calculated strain recovery efficiency at 30 % strain ( $N = 4$  samples tested per condition). Each point denotes a measurement on a different sample, and bar plot shows mean value with error bars denoting standard error of the mean (SEM). One-way ANOVA test for statistics \*  $p < 0.05$ , \*\*  $p < 0.01$

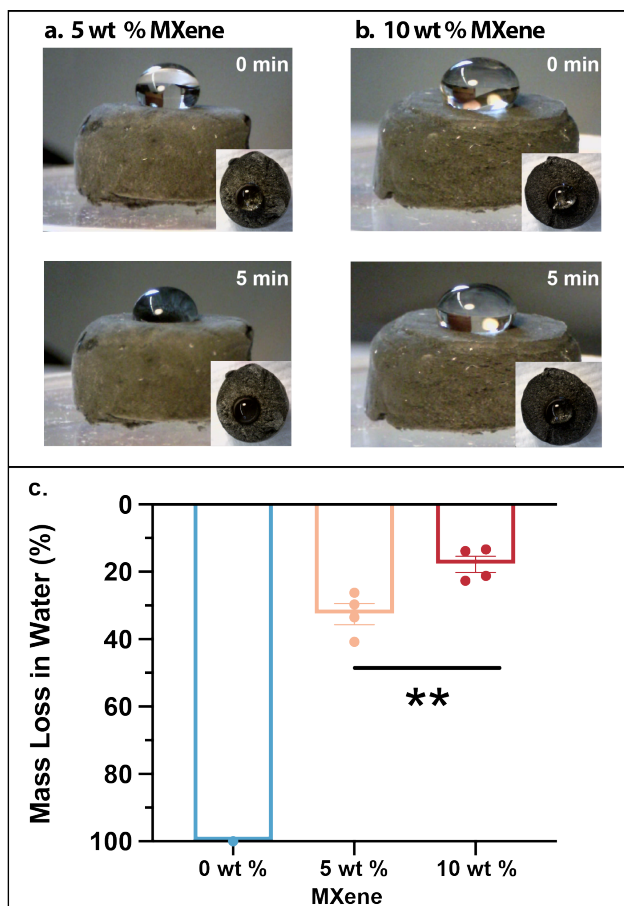


Figure S4: Water stability of MXene-silk aerogels. (a, b) Water droplet to demonstrate stability for 5 wt % and 10 wt % MXene aerogels, timed images over 5 minutes. (c) Percent of mass loss for 5 wt % and 10 wt % MXene aerogel measured after 5 days ( $N = 3$  samples), Student's t-test for statistics \*  $p < 0.05$ , \*\*  $p < 0.01$ . Silk-only aerogels were fully dissolved after 5 days in water and counted as 100% mass loss.

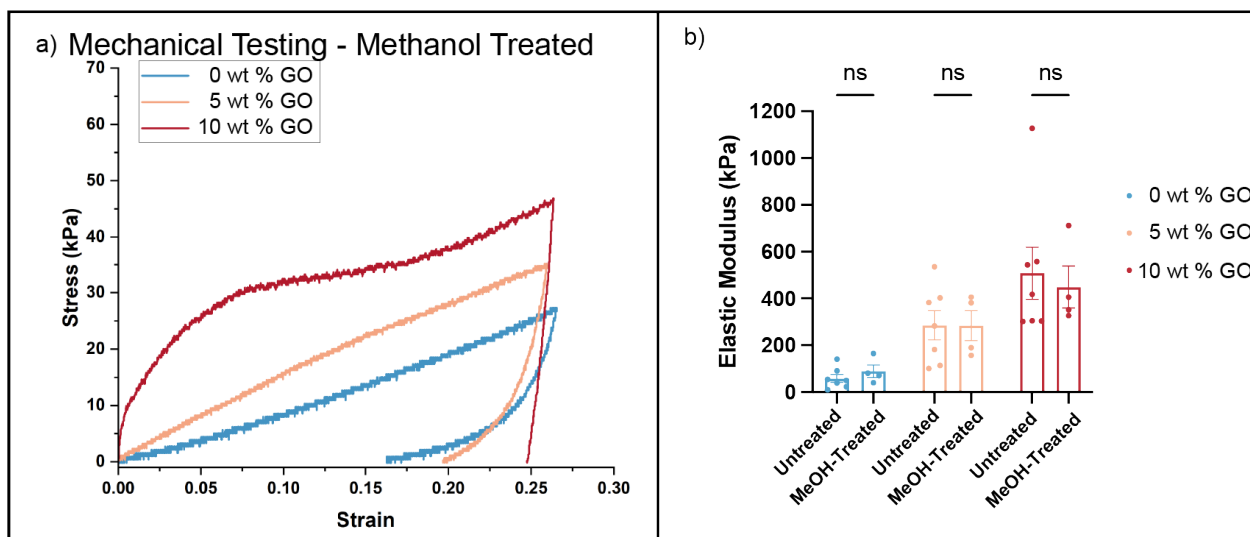


Figure S5: Mechanical testing of methanol-treated silk-GO aerogels. a) Representative stress and strain curves from compression testing on silk aerogels (0, 5, 10 wt % GO) after methanol treatment. b) Calculated elastic modulus for untreated ( $N = 5$  samples) and methanol-treated aerogels (MeOH) ( $N = 4$  samples). Plotted in a box-and-whisker plot as  $x$ =median value and whisker=standard error of the mean (SEM). Two-way ANOVA test for statistics \*  $p < 0.05$ , \*\*  $p < 0.01$ .

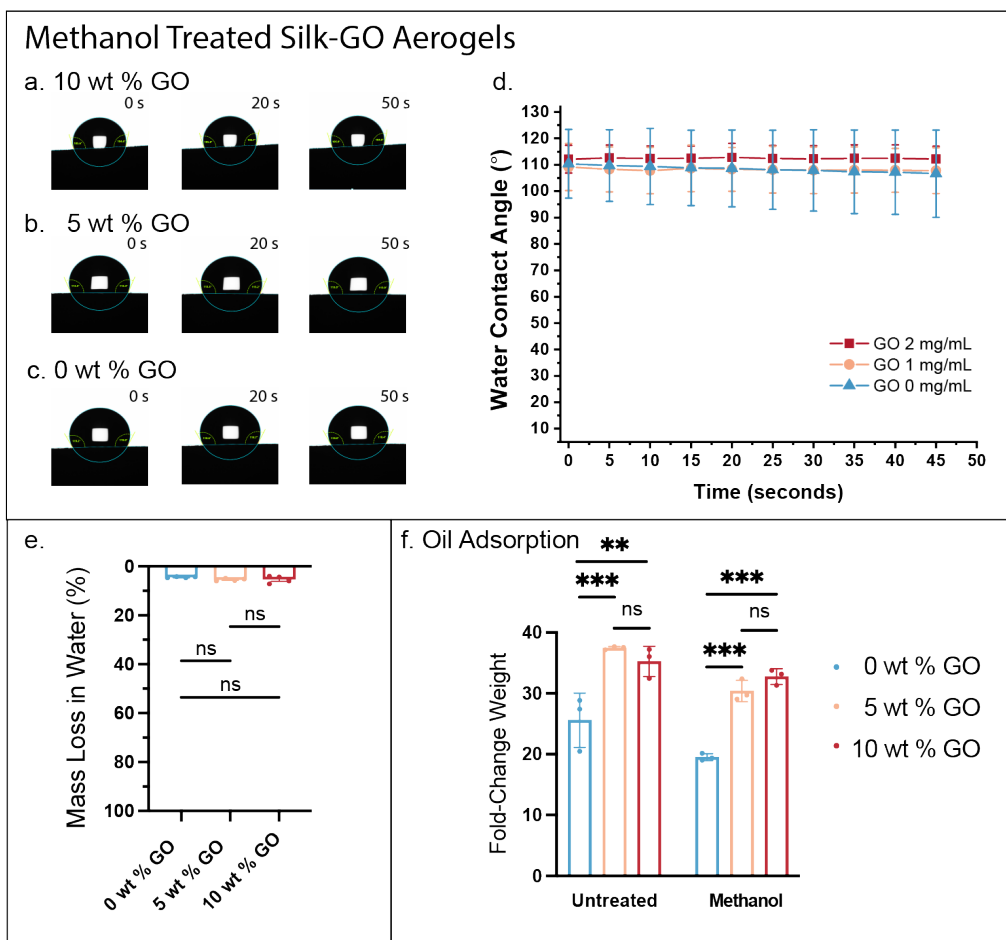


Figure S6: Interactions of methanol-treated silk-GO aerogels with water. (a-c) Representative water contact angle for silk aerogels (10, 5, 0 wt % GO). (d) Average contact angle of water after contacting aerogel surface ( $N = 3$  samples). (e) Percentage of mass loss for all concentrations for methanol treated aerogels, plotted in a bar plot as  $x$ =median value and whisker=standard error of the mean (SEM) ( $N = 4$  samples), One-way ANOVA test. (f) Measured naphthenic oil absorption for methanol treated aerogels (fold change by weight), plotted in a bar plot as  $x$ =mean value and error bars are standard error of the mean (SEM) ( $N=4$ ). Two-way ANOVA test, \*  $p < 0.05$ , \*\*  $p < 0.01$ .

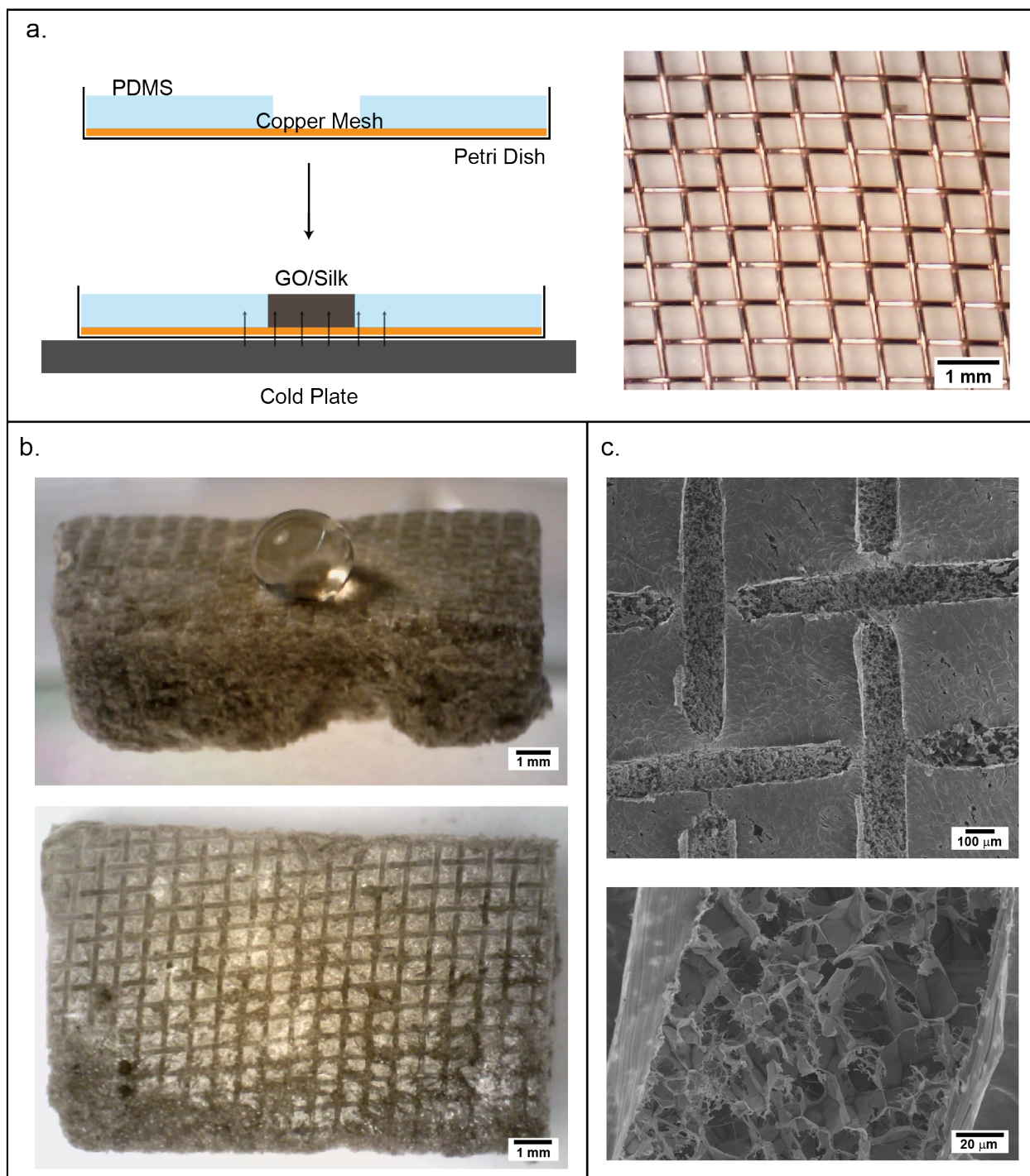


Figure S7: Large area deposition of silk-GO aerogels. a) Schematic of experimental setup and representative image of pristine copper mesh. (b) Cross-section and top-down view of silk aerogel with 10 wt% GO after casting on a copper mesh. Water droplet added in cross sectional view to illustrate hydrophobic properties. (c) SEM of aerogel surface after casting on copper mesh.